

Electrochemical treatment of waters with BDD anodes: kinetics of the reactions involving chlorides

A. M. Polcaro · A. Vacca · M. Mascia ·
S. Palmas · J. Rodriguez Ruiz

Received: 23 September 2008 / Accepted: 6 March 2009 / Published online: 1 April 2009
© Springer Science+Business Media B.V. 2009

Abstract In this work the products of the oxidation at BDD anode of chloride ions in aqueous solutions were identified during galvanostatic electrolyses performed in a filter-press reactor operating both in batch and continuous mode. A set of experiments were performed in order to study the effect of operating conditions (current density, residence time, hydrodynamics and chloride concentration) on distribution and concentration of electrolysis by-products. As a comparison experiments were also performed using a commercial DSA anode. A simple mathematical model was formulated, and the model predictions agree with the experimental data in a wide range of experimental conditions. The results of this work showed that at low chloride concentrations electrolysis with BDD anode produce a mixture of powerful oxidant: low current density, high mass transfer conditions and low residence time were found as optimal conditions to maximize the concentration of oxidants and minimize the concentration of chlorates. The proposed reaction mechanism may also justify the controversial effect of chloride ions in wastewater treatments: the electrolysis carried out with BDD anodes and electrolyte containing chloride concentration higher 1 g/L could meet the target of the process only if the active chlorine is effective in oxidation of the pollutant that must be removed.

Keywords Active chlorine · BDD electrode · Disinfection by-products · Reactive oxygen species

List of symbols

A_a	Anode area (m^2)
A_c	Cathode area (m^2)
V_R	Reactor volume (m^3)
C_i	Concentration of the i th compound ($mol\ m^{-3}$)
Q	Inlet–outlet flow rate (continuous mode) ($m^3\ s^{-1}$)
Q_R	Recirculating flow rate ($m^3\ s^{-1}$)
D_i	Diffusivity of the i th compound ($m^2\ s^{-1}$)
F	Faraday number ($C\ mol^{-1}$)
i	Anodic current density ($mA\ cm^{-2}$)
i_{lim}	Limiting anodic current density ($mA\ cm^{-2}$)
I	Current intensity (mA)
k_m	Mass transfer coefficient ($m\ s^{-1}$)
K_d	Specific reaction rate for oxidant decay (s^{-1})
κ	Volume of liquid related to a mole of OH radical ($m^3\ mol^{-1}$)
n_i	Number of moles of the i th specie
δ	Diffusion layer thickness $\delta = \frac{D_i}{k_m}$ (m)
τ	Residence time $\tau = \frac{V_R}{Q}$ (s)
ε	Faradic yield in continuous mode experiments
η	Faradic yield in batch mode experiments

1 Introduction

The electrochemical treatments of waters with boron doped diamond (BDD) have shown a great effectiveness for several purposes such as wastewater treatments [1, 2], disinfection or purification of groundwater and natural waters [3, 4]. A large number of scientific publications have also appeared regarding the treatment of synthetic and real wastewaters containing either inorganic and/or organic compounds [5].

As the organic oxidation is concerned, it is well established that the great effectiveness of BDD is due to the

A. M. Polcaro (✉) · A. Vacca · M. Mascia ·
S. Palmas · J. Rodriguez Ruiz
Dipartimento di Ingegneria Chimica e Materiali,
University of Cagliari, P.zza d'Armi, Cagliari, Italy
e-mail: polcaro@dicm.unica.it

generation of hydroxyl radicals from water oxidation. OH radicals may oxidize the organics in either one or multiple stages often leading to mineralization. Hydroxyl radicals are high reactive, and they may oxidize the organic compounds only in a thin reaction layer adjacent to the anodic surface so that the organic removal is a pseudo surface process often mass transfer controlled [2].

It was also proposed that the hydroxyl radicals can form such reactive oxygen species, ozone and hydrogen peroxide which may react with the organic matter in the solution bulk through mediated oxidation processes [6]. Moreover if the water contains sulphate or phosphate ions, peroxodisulphate and peroxodiphosphate may be formed; also these oxidants can contribute to the oxidation in the bulk solution [7, 8].

Depending on nature of the organics, water composition and operative conditions, the process may be controlled by one or more steps which can lead to different performances of BDD anodes.

The effect of chloride ions was investigated in several papers which were devoted to disinfection and purification of water, as well as to wastewater treatment, and a particular behaviour was observed. If the chloride are present in low concentration, as usual in natural waters, the disinfection or purification processes are mediated by active chlorine electrogenerated (HClO/ClO^- and ClO_2), but it is also possible the formation of chlorite, chlorate and perchlorate ions which are undesired disinfection by-products [9].

In the case of application of BDD anode in the wastewater treatment, the effect of chloride ions is controversial: some studies reported that an increase of the chloride concentration causes an increase of the overall oxidation rate indicating that the active chlorine produced at the anode can give a bulk contribution [10]. Other researches found that the addition of chloride ions at the solution causes a decrease in the removal efficiency of COD [11].

Since the real application of the electrochemical treatment using BDD anodes both for wastewater treatment and disinfection of natural waters, is strictly related to the knowledge of the fate of chloride ions, further studies are needed in order to better clarify this topic.

In this work the products of the oxidation at BDD anode of chloride ions in aqueous solutions were identified during galvanostatic electrolyses performed in a filter-press reactor operating both in batch and continuous mode. Particular attention was paid on the effect of such operating conditions, current density, residence time, hydrodynamics and chloride concentration on distribution and concentration of electrolysis by-products. As a comparison experiments were also performed using a commercial DSA anode.

Moreover, on the basis of the experimental data, a reaction mechanism for chloride oxidation at BDD anode has been proposed.

2 Materials and methods

2.1 Experimental apparatus

Electrolyses were performed in a single compartment filter press cell (EC Electro MP-Cell) with two parallel electrodes spaced 0.5 cm. The cell was inserted in a hydraulic circuit, showed in Fig. 1. The electrolyte was pumped by a centrifugal pump from the reservoir to the cell and back in a closed loop. The volume of the electrolyte was 850 cm^3 and the recirculating flow rate (Q_R) ranged from 0.45 to $1.4 \text{ dm}^3 \text{ min}^{-1}$.

The anodic materials were a circular p-type semiconducting boron-doped diamond (B concentration in the range 3500–5000 ppm), supplied by ADAMANT and a commercial $\text{Ti}/\text{Ru}_{0.3}\text{Ti}_{0.7}\text{O}_2$ electrode supplied by DENORA. The cathode was a stainless steel (AISI 304) circle. The anodic and cathodic area were 80 and 25 cm^2 respectively.

2.2 Mass transfer characterisation

To characterize the mass transfer behaviour of the cell, the well established limiting-current technique was adopted, so that the value of mass transfer coefficient (k_m) was derived (Eq. 1) from the limiting current i_L , measured at the working electrode when the mass transfer conditions were achieved:

$$k_m = \frac{i_L}{zFC^b} \quad (1)$$

z is the number of electrons involved in the process, F is the Faraday number ($F = 96500 \text{ C/eq}$) and C^b is the concentration of the reactant in the bulk solution.

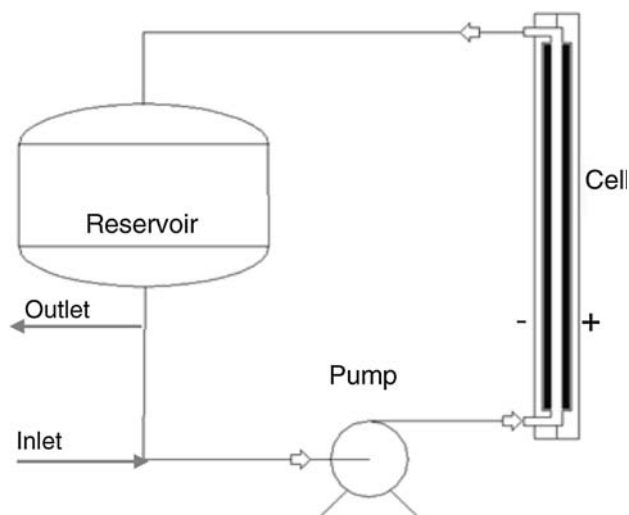


Fig. 1 Experimental set up

In the specific case mass transfer coefficients were determined by evaluating the related limiting current densities for the ferro/ferricyanide redox couple (supporting electrolyte 0.5 M Na₂CO₃). In particular, the determination of the anodic mass transfer coefficient (k_m^a) was made by measuring the limiting current densities for K₄Fe(CN)₆ 1 mM oxidation in presence of an excess of K₃Fe(CN)₆ (0.1 M) in order to ensure that the cathodic reaction never became the limiting process. Analogously, an excess of K₄Fe(CN)₆ was guaranteed during measurements of the cathodic mass transfer coefficient (k_m^c) [12]. Negligible differences were found between the values of anodic and cathodic mass transfer coefficients in the relevant conditions. Under the experimental conditions adopted in this work, the following values were obtained: $k_m = 0.3 \times 10^{-5} \text{ m s}^{-1}$ ($Q_R = 0.45 \text{ dm}^3 \text{ s}^{-1}$); $k_m = 0.7 \times 10^{-5} \text{ m s}^{-1}$ ($Q_R = 0.55 \text{ dm}^3 \text{ s}^{-1}$); $k_m = 1.2 \times 10^{-5} \text{ m s}^{-1}$ ($Q_R = 1.4 \text{ dm}^3 \text{ s}^{-1}$).

By assuming the same value of dynamic viscosity for the diluted aqueous solutions, the values of mass transfer coefficients for the *i*th specie (k_{mi}) may be evaluated from the value obtained for the ferro/ferricyanide redox couple (k_{m0}), at the relevant Reynolds number [13].

$$k_{mi} = k_{m0} \left[\frac{D_i}{D_0} \right]^{\frac{2}{3}} \quad (2)$$

where D_i and D_0 are the relevant diffusion coefficients.

2.3 Experiments

The runs were performed both in batch and continuous mode. In the continuous runs the inlet and outlet flow rates (Q) were fixed in the range 0.05–0.4 dm³ min⁻¹ by a peristaltic pump. The residence times in the electrochemical system can be evaluated as:

$$\tau = \frac{V_r}{Q} \quad (3)$$

Under the experimental conditions adopted in this work, τ ranged from 2 to 16 min.

The electrolyses were performed by imposing anodic current density values ranging from 2.5 to 7.6 mA cm⁻² by means of a galvanostat (AMEL—2049). All the experiments were carried out with solutions containing 200 mg dm⁻³ of SO₄²⁻ as supporting electrolyte and different amount of Cl⁻ ranging from 50 to 2500 mg dm⁻³.

2.4 Analysis

During the runs samples were withdrawn and analysed for the concentration of reactant and products: since some components may have very short live times, the analysis were done immediately after sampling. The oxidant

concentrations expressed as mg dm⁻³ of active chlorine were measured by the DPD method, hypochlorite concentration was determined by spectrophotometric analysis at 294 nm, chlorine dioxide was measured spectrophotometrically by red chlorophenol method [14]. (Spectrophotometer VARIAN—Cary 50). Ion concentrations were measured by a Metrohm compact ion chromatograph 761 equipped with a conductivity detector and 6.1006.430 Metrosep Anion supp. 4 column, (mobile phase 2 mM NaHCO₃/1.3 mM Na₂CO₃, flow rate 1.5 cm³ min⁻¹).

In particular, ion chromatography was effectively used to measure the concentration of Cl⁻, ClO₃⁻ and ClO₄⁻ as well as possible variations in the SO₄⁻ concentration. Analyte identification was accomplished on the basis of the retention times of the analytes and the quantification was performed by external calibration. As far as the concentration of hypochlorite is concerned, some problems arose since chloride and hypochlorite have overlapping peaks. As suggested by Bergmann [15], the analysis was carried out twice with and without hypochlorite elimination and the corresponding concentration values calculated by solving a mathematical system of equations. Indication on the actual concentration of hypochlorite was also derived from the UV spectrum measurements (ClO⁻ absorption peak at 294 nm) at least when its concentration was greater than 2–3 ppm.

DPD method gave a measure of the active chlorine, as global concentration of oxidising species contained in the sample: ClO⁻/HClO, ClO₂, but also H₂O₂, O₃ and per-sulphate can be evaluated with this measure. In our case, most of the oxidant is constituted by ClO⁻/HClO as demonstrated by the analysis of analogous samples performed with DPD method and UV spectrum.

3 Results and discussion

The galvanostatic electrolyses ad BDD and DSA anodes in dilute solutions of chloride have produced different results: at DSA the oxidizing species detected by DPD method are mainly constituted by hypochlorite while at BDD a mixture of oxidizing species containing hypochlorite, chlorine dioxide and Reactive Oxygen Species (ROS) may be formed [15]; moreover, the oxidants produced at BDD were less stabile than those at DSA.

This behaviour could be justified considering that the different species produced at BDD anode can react with each other leading to a fast decay of the oxidant concentration. In order to quantify this decay, continuous electrolyses were carried out until the steady state was reached: feed flow rate and current were then interrupted, and the trend with time of oxidant concentration was monitored. An example is showed in Fig. 2: at steady state the inlet solution contained 100 ppm of chloride ions, the

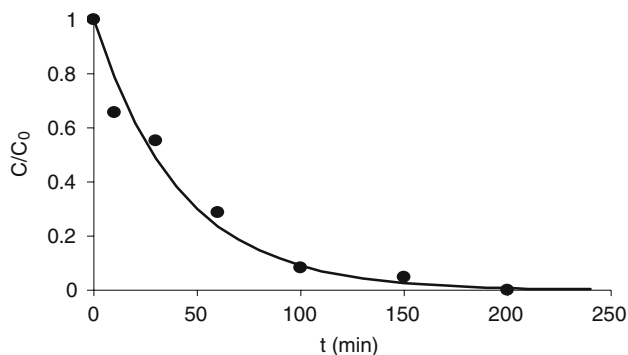


Fig. 2 Trend with time of oxidizing species concentration, normalised with respect to the initial concentration ($C_{OX}^0 = 6.2 \text{ mgCl}_2 \text{ dm}^{-3}$): the initial solution was obtained by continuous electrolysis at BDD with an inlet solution containing $C_{Cl^-}^0 = 100 \text{ mg dm}^{-3}$ at $i = 5 \text{ mA cm}^{-2}$, $\tau = 16 \text{ min}$, $Q_R = 1.4 \text{ dm}^3 \text{ min}^{-1}$

outlet contained $6.2 \text{ mgCl}_2/\text{L}$, the anodic current density was 5 mA cm^{-2} . The decay of oxidants may be interpreted by a pseudo-first order kinetic with an apparent rate constant equal to $4 \times 10^{-4} \text{ s}^{-1}$.

Figure 3a–c show the trend with electrolysis time of the concentration of chloride and by-products, normalized with respect to the initial concentration of chloride, formed during experiments with DSA or BDD anode in batch mode. As can be seen the behaviour at two electrodes is different: the decrease of chloride concentration with time is faster at BDD anodes and chlorate ions are formed. At DSA less than 1 ppm of chlorates was found.

The figure also shows that the concentration of oxidants is higher at the lower values of the recirculating flow rate in the electrolyses with DSA anodes. This result may be explained considering that in the undivided cell used in the experiments oxidants may be reduced to chlorides at the stainless steel cathode through an electrochemical reaction, which competes with the main cathodic reaction of hydrogen evolution. The cathodic reduction of oxidants is a fast electrochemical reaction, so that the whole reduction

process is mass transfer controlled. An increase of recirculating flow rate increases the reaction rate of oxidant reduction.

Different results were found during experiments with BDD: high recirculating flow rate leads to higher oxidant concentrations suggesting the presence of different and more complex reaction mechanisms, as it will be discussed in the following part of this paper.

The effect of the initial chloride concentration on the composition of the treated solution using BDD anode is reported in Fig. 3a–b. As can be observed an increase in the initial chloride concentration causes a different distribution of oxidation products: in particular the chlorate concentration decreases as the concentration of chloride initially present in the solution increases.

Moreover the system is less sensitive to the recirculating flow rate at high chloride concentrations.

Figure 4 shows the mean faradic yield for the oxidation of chloride ions at BDD and DSA anodes obtained for different initial chloride concentrations in the initial stage of the treatment (10 min), the operative conditions being the same. The faradic yield for the anodic oxidation of chlorides was evaluated by the balance (Eq. 4), between the consumption of chlorides by the anodic reaction and its production by cathodic reduction and chemical decay of hypochlorite.

$$V_r \frac{d[Cl^-]}{dt} = \eta \frac{I}{2F} - A_c k_m [HClO] - V_r K'_d [HClO] \quad (4)$$

The faradic yield can be obtained from Eq. 4:

$$\eta = \frac{V([\text{Cl}^-]_{t+\Delta t} - [\text{Cl}^-]_t) / \Delta t + A_c k_m [HClO] + V_r K'_d [HClO]}{I/2F} \quad (5)$$

As can be seen the faradic yield increases as the initial concentration of chloride increases for both electrodes, but at BDD is higher than that at DSA for each initial

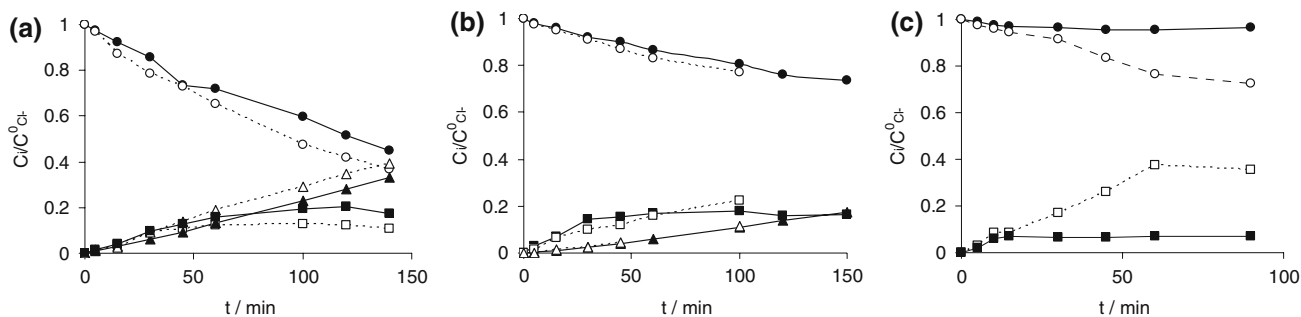


Fig. 3 Trend with time of chloride (●○), chlorate (▲△) and oxidizing species (■□) concentrations normalized with respect to the initial concentration of chloride ions, during batch electrolysis at $i = 5 \text{ mA cm}^{-2}$, under different experimental conditions: dotted

line $Q_R = 0.45 \text{ dm}^3 \text{ min}^{-1}$, full line $Q_R = 1.4 \text{ dm}^3 \text{ min}^{-1}$. **a** BDD, $C_{Cl^-}^0 = 100 \text{ mg dm}^{-3}$; **b** BDD, $C_{Cl^-}^0 = 600 \text{ mg dm}^{-3}$; **c** DSA, $C_{Cl^-}^0 = 100 \text{ mg dm}^{-3}$

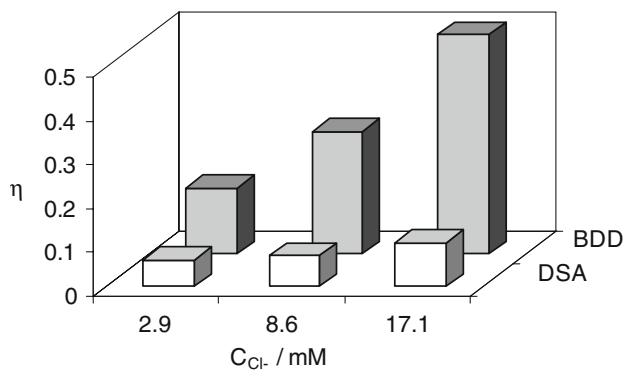


Fig. 4 Faradic yield η of chloride oxidation from batch electrolysis with different initial chloride concentrations; $i = 5 \text{ mA cm}^{-2}$, $Q_R = 1.4 \text{ dm}^3 \text{ min}^{-1}$

concentrations. Moreover at BDD anode the effect of the chloride concentration on the faradic yield is more evident.

This behaviour may be interpreted considering the competition between chloride oxidation and oxygen evolution at the two electrodes, current density value being the same. Since at DSA anode the oxygen evolution takes place at low overpotential [16], this reaction is highly competitive with chlorides oxidation. On the other hand, the overpotential for the oxygen evolution is very high at BDD, so that the oxidation of chlorides is kinetically favoured [17]. This can be seen from pseudo steady state polarization curves obtained (at 0.5 mV s^{-1}) with different chloride concentration at BDD anode (Fig. 5): with 30 mM of chlorides the onset of the chlorine evolution shifts to less positive potential than that required for oxygen evolution.

The results of continuous electrolyses with BDD anodes are reported in table 1, which summarises the operative conditions and the relevant results. Current density and residence time were adjusted to obtain low conversion of chloride ions ($X < 1\%$) in order to highlight the effect of their concentration in the inlet stream. As can be seen, experiments show that oxidants and chlorate are the main products in the outlet stream, chlorites were found at detectable concentration only at high residence time. Results show also that perchlorate ions were not detected in the electrolyses under the experimental conditions adopted in this work. As already observed in the discussion of the results obtained in batch experiments, also in continuous mode the increase of the recirculating flow rate results in a decrease of steady state values of chlorates concentration and in an increase of the values of oxidizing species, while an increase of current density and residence time leads to high chlorate concentration, mainly at low recirculating flow rate. Moreover high values of chloride ions concentration in the inlet stream result in very low chlorate concentrations in the outlet stream.

The faradic yield (Eq. 6) for the oxidation of chloride to form hypochlorous acid may be calculated from the mole

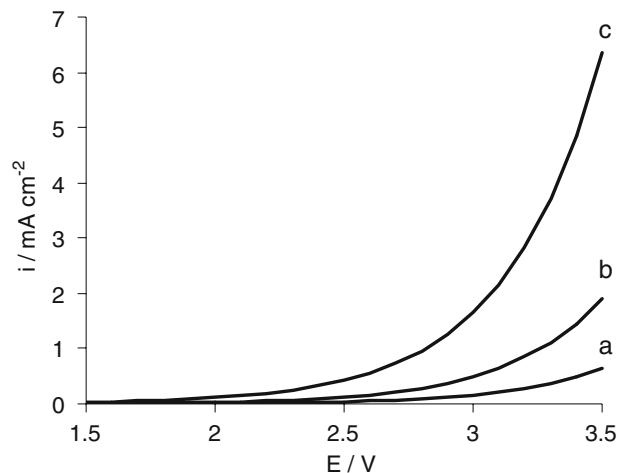


Fig. 5 Polarization curves at BDD anode of aqueous solution with different composition. **a** Na_2SO_4 1.5 mM; **(b)** Na_2SO_4 1.5 mM + NaCl 15 mM; **(c)** Na_2SO_4 1.5 mM + NaCl 30 mM. Scan rate 0.5 mV s^{-1} ; values of potential are referred to SCE

balance in continuous mode at different chloride concentrations; values are reported in Fig. 6.

$$\varepsilon = \frac{Q([\text{Cl}^-]^{in} - [\text{Cl}^-]^{out})_{s.s.} + A_c k_m [\text{HClO}]_{s.s.} + V_r K'_d [\text{HClO}]_{s.s.}}{I/2F} \tag{6}$$

As can be seen the faradic yield tends to 1 as the chloride concentration increases, indicating that at high chloride concentrations (60 mM) the current is mainly dedicated to chlorine evolution.

The empirical Eq. 7 was used to fit the experimental data of the faradic yield as a function of chloride concentration:

$$\varepsilon = \frac{a[\text{Cl}^-]}{1 + b[\text{Cl}^-]} \tag{7}$$

Parameters a and b should depend on the current density: however the range of anodic current density adopted in this work is narrow (from 2.5 to 7.6 mA cm^{-2}) and this dependence was neglected. Under this approximation, constant values of $a = 0.05$ and $b = 0.04$ were found to give the best agreement between experimental and calculated data.

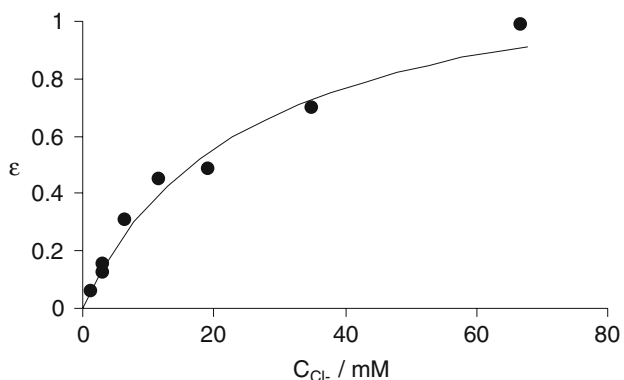
As the reactions occurring during the process are concerned, it is well known from the literature that the OH radicals weakly sorbed at the electrode surface are formed in the first step of water oxidation [18].



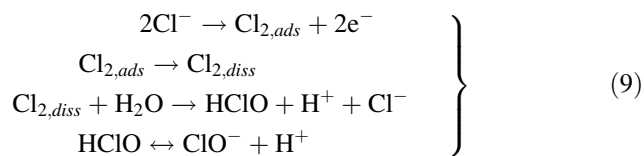
Chloride ions may react in a complex manner to give adsorbed chlorine (although weakly sorbed at the electrode surface) and dissolved chlorine, which reacts with water to hypochlorous acid and hypochlorite [19]. The distribution

Table 1 Operative conditions and relevant results for continuous electrolyses with BDD anodes

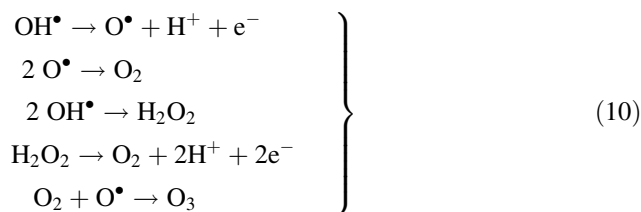
Residence time (τ min)	Recirculating flow rate Q_R ($\text{dm}^3 \text{min}^{-1}$)	Anodic current density (i mA cm^{-2})	$[\text{Cl}^-]$ (mg dm^{-3})	Oxidants (DPD test) ($\text{mgCl}_2 \text{dm}^{-3}$)	$[\text{ClO}_2^-]$ (mg dm^{-3})	$[\text{ClO}_3^-]$ (mg dm^{-3})
2	1.4	5.0	117	1.1	–	2.0
4	1.4	3.7	119	1.4	–	3.0
4	1.4	5.6	120	2.2	–	4.6
4	1.4	2.5	121	1.4	0.07	1.8
4	0.45	2.5	125	0.9	–	2.0
4	0.45	5.6	126	1.4	–	5.0
4	1.4	3.7	446	6.9	0.06	4.1
8.5	1.4	5.0	119	3.0	0.07	8.0
16	1.4	3.7	55	1.7	–	7.6
16	1.4	3.7	119	4.5	–	11.8
16	1.4	2.5	124	4.0	–	7.7
16	0.45	2.5	125	2.8	0.05	9.0
16	0.45	5.0	125	6.2	0.04	19.3
16	1.4	5.6	127	7.5	–	17.2
16	1.4	3.7	256	18.0	0.17	19.3
16	1.4	3.7	446	26.0	0.25	19.5
16	0.45	7.5	447	30.0	0.30	40.0
16	1.4	3.7	711	29.8	0.54	15.3
16	1.4	3.7	1260	43.5	0.90	13.1
16	1.4	3.7	2450	55.0	1.40	11.0

**Fig. 6** Faradic yield ε of chloride oxidation in galvanostatic electrolysis in continuous mode for different inlet chloride concentrations at $i = 5 \text{ mA cm}^{-2}$, $Q_R = 1.4 \text{ dm}^3 \text{min}^{-1}$, $\tau = 16 \text{ min}$

between the three main active chlorine components is strongly dependent on pH.

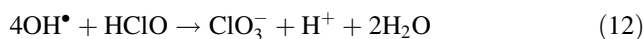
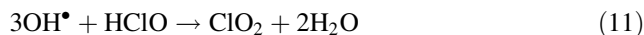


Oxygen can be formed by a series of reactions involving radical species obtained from the first step of water oxidation at the anode surface [20]:



As can be seen it is also possible the formation of ROS.

In our experiments, chlorine dioxide and chlorate were always found in the samples obtained at BDD anodes while at DSA these species were not detected. On the basis of this result, the oxidation of chlorine from hypochlorite to chlorine dioxide and chlorate is expected to occur by reaction with OH radicals, rather than by direct electrochemical reaction [14].



Chlorite can be also formed, but only traces of this species were detected during the runs: this indicates that chlorites can rapidly react to chlorates, as it was suggested from the literature [14].

A simplified mathematical model was then implemented to quantitatively interpret the kinetics of the process. Although the anode mechanism is rather complex, different assumption were done, based on the experimental results

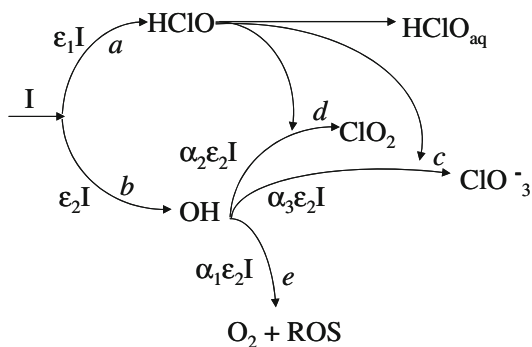


Fig. 7 Scheme of the anodic reactions at BDD anodes: (a) electrochemical chloride oxidation, (b) formation of hydroxyl radicals by water discharge, (c) formation of chlorate ions—reaction 12, (d) formation of chlorine dioxide—reaction 11, (e) oxygen evolution and formation of ROS—reaction 10

discussed above: Fig. 7 summarises the reaction pathway considered in the model to represent the anode processes.

In Fig. 7 $\epsilon_1 I$ is the current of chloride oxidation, $\epsilon_2 I$ is the current for generation of OH radicals, and α_2 and α_3 are the fractions of OH radicals used to form chlorine dioxide and chlorate, respectively.

The deactivation of active chlorine in liquid phase experimentally observed may be due to different mechanisms, such as reactions with ROS and disproportionation of chlorine dioxide which leads to the formation of chlorate and chlorite [21].



As it is well known, the disproportionation of ClO_2^- to give chlorite and chlorate is very slow at 25 °C, and this contribution was neglected in the model.

The mole balances of the model were written for the steady state considering the electrochemical reactor with two zones adjacent to the electrode surfaces and a third zone corresponding to the bulk. The low ratio between the inlet flow rate and the recirculating flow rate and the low conversion per pass, allows to represent the cell as a combination of three CSTR: two reactors simulate the cathodic and the anodic films whereas the third corresponds to the bulk of the solution. A mass transfer process occur between each electrode film and the bulk.

The volume of anodic and cathodic zones (V_f) depends on the thickness of the Nernst diffusion layer δ , ($V_f = A \cdot \delta$) evaluated from the mass transfer coefficient (k_m) and the diffusivity (D):

$$\delta = \frac{D}{k_m} \tag{15}$$

The volume of the bulk solution zone is equal to the overall recirculating volume.

In the anodic zone the electrochemical reaction at the electrode surfaces (Eqs. 8–10) and the chemical reactions in liquid phase (Eqs. 11–14) occur, in the cathodic zone along with the main reaction of hydrogen evolution, the reduction of oxidant species takes place, whereas in the bulk solution zone only the chemical reaction (Eqs. 13–14) can occur.

As the kinetics is concerned, on the bases of the proposed reaction mechanism the following equations can be written:

– Anode reactions

$$\frac{dn_{HClO}}{dt} = \frac{\epsilon_1 I}{2F} \tag{16}$$

$$\frac{dn_{OH}}{dt} = \frac{\epsilon_2 I}{F} \tag{17}$$

$$\frac{dn_{ClO_2}}{dt} = \kappa \frac{\alpha_2 \epsilon_2 I}{F} [HClO] \tag{18}$$

$$\frac{dn_{ClO_3^-}}{dt} = \kappa \frac{\alpha_3 \epsilon_2 I}{F} [HClO] \tag{19}$$

where κ ($m^3 \text{ mol}^{-1}$) is the volume of liquid film related to a mole of OH radicals.

– Decay of oxidants in the anodic zone

$$-\frac{dn_{HClO}}{dt} = V_f K'_d [HClO] \tag{20}$$

$$-\frac{dn_{ClO_2}}{dt} = V_f K''_d [ClO_2] \tag{21}$$

In the bulk solution only the reactions of decay of oxidant were considered:

$$-\frac{dn_{HClO}}{dt} = V_r K'_d [HClO] \tag{22}$$

$$-\frac{dn_{ClO_2}}{dt} = V_r K''_d [ClO_2] \tag{23}$$

At the cathode surface, reduction of oxidants and hydrogen evolution may take place. Reduction of oxidants is expected to be a fast electrochemical reaction, so that the kinetics of the process was assumed under mass transfer control.

$$-\frac{dn_{HClO}}{dt} = A_c k'_m [HClO] \tag{24}$$

$$-\frac{dn_{ClO_2}}{dt} = A_c k''_m [ClO_2] \tag{25}$$

The model equations are constituted by the mole balances of hypochlorite, chlorine dioxide and chlorates in each zone; in a continuous system at the steady state we can write:

– Anodic zone

$$\frac{\epsilon_1 I}{2F} - \kappa(\alpha_2 + \alpha_3) \frac{\epsilon_2 I}{F} [HClO]_f - K'_d V_f [HClO]_f - A_a k'_m ([HClO]_f - [HClO]_b) = 0 \tag{26}$$

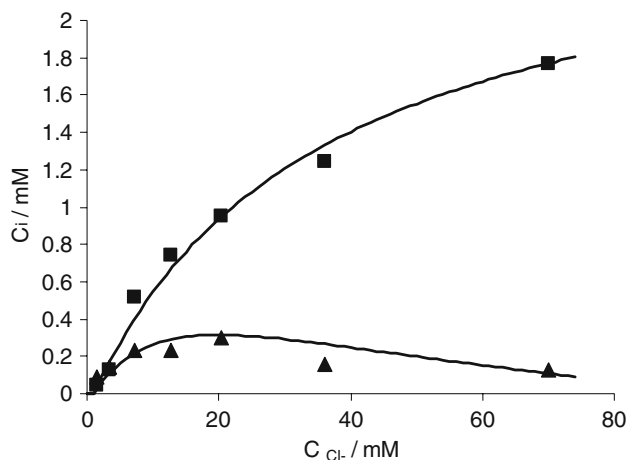


Fig. 8 Comparison between calculated (full lines) and experimental concentrations of oxidants (■) and chlorates (▲) in the outlet stream as a function of chloride concentrations from continuous electrolyses ($i = 3.8 \text{ mA cm}^{-2}$, $\tau = 16 \text{ min}$, $Q_R = 1.4 \text{ L/min}$)

$$\kappa \frac{\alpha_2 \varepsilon_2 I}{F} [\text{HClO}]_f - V_f K_d'' [\text{ClO}_2]_f - A_a k_m'' \left([\text{ClO}_2]_f - [\text{ClO}_2]_b \right) = 0 \quad (27)$$

$$\kappa \frac{\alpha_3 \varepsilon_2 I}{F} [\text{HClO}]_f + V_f K_d'' [\text{ClO}_2]_f - A_a k_m''' \left([\text{ClO}_3^-]_f - [\text{ClO}_3^-]_b \right) = 0 \quad (28)$$

– bulk zone

$$A_a k_m' \left([\text{HClO}]_f - [\text{HClO}]_b \right) - A_c k_m' [\text{HClO}]_b - K_d' V_r [\text{HClO}]_b - Q [\text{HClO}]_b = 0 \quad (29)$$

$$A_a k_m'' \left([\text{ClO}_2]_f - [\text{ClO}_2]_b \right) - V_r K_d'' [\text{ClO}_2]_b - A_c k_m'' [\text{ClO}_2]_b - Q [\text{ClO}_2]_b = 0 \quad (30)$$

$$A_a k_m''' \left([\text{ClO}_3^-]_f - [\text{ClO}_3^-]_b \right) + V_r K_d'' [\text{ClO}_2]_b - Q [\text{ClO}_3^-]_b = 0 \quad (31)$$

Fig. 9 Comparison between calculated and experimental concentrations of chlorates (a) and oxidants (b) in the outlet stream at $\tau = 16 \text{ min}$ as a function of the imposed current intensity at different experimental conditions:
 $C_{\text{Cl}^-} = 3.4 \text{ mM}$ (□)
 $Q_R = 0.45 \text{ dm}^3 \text{ min}^{-1}$ (■)
 $Q_R = 1.4 \text{ dm}^3 \text{ min}^{-1}$;
 $C_{\text{Cl}^-} = 12 \text{ mM}$ (○)
 $Q_R = 0.45 \text{ dm}^3 \text{ min}^{-1}$ (●)
 $Q_R = 1.4 \text{ dm}^3 \text{ min}^{-1}$ (●)

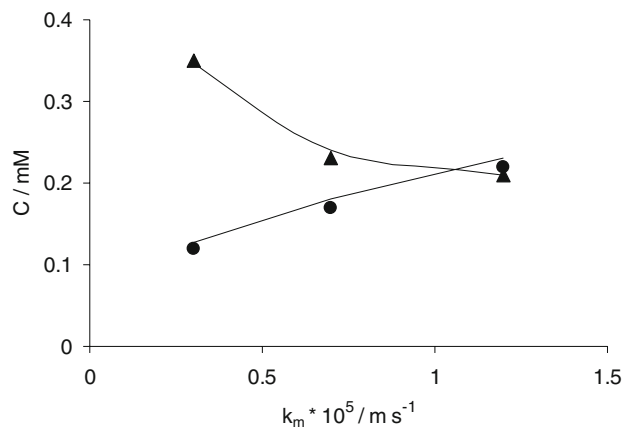
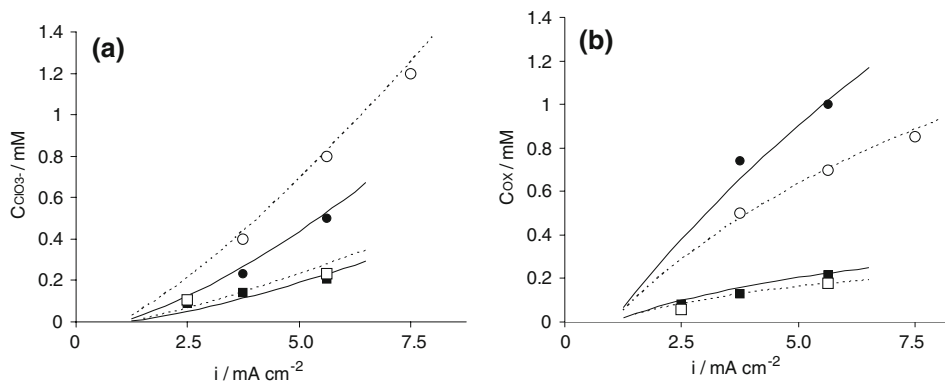


Fig. 10 Model predictions and experimental data for the concentrations of oxidant (●) and chlorates (▲) in the outlet stream of continuous electrolyses under different mass transfer conditions. $C_{\text{Cl}^-} = 3.4 \text{ mM}$, $\tau = 16 \text{ min}$, $i = 3.8 \text{ mA cm}^{-2}$

In the model Eqs. 26–31, the reaction rate constants $\alpha_2 \kappa$, $\alpha_3 \kappa$, K_d' , K_d'' were the only adjustable parameters. The set of algebraic Eqs. 26–31 was solved to obtain the concentration of hypochlorite, chlorate and chlorine dioxide in the outlet stream of the steady state reactor.

Values of $\alpha_2 \kappa = 1 \times 10^{-3} \text{ m}^3 \text{ mol}^{-1}$, $\alpha_3 \kappa = 1 \times 10^{-2} \text{ m}^3 \text{ mol}^{-1}$, $K_d' = 8 \times 10^{-4} \text{ s}^{-1}$ and $K_d'' = 2 \times 10^{-3} \text{ s}^{-1}$ gave the best agreement between experimental and calculated data.

The following figures show a comparison between experimental and model predicted data of concentration of active chlorine and chlorate ions. As can be seen a good agreement between experimental and model-predicted data has been obtained.

Figure 8 shows the effect of the concentration of chloride ions on the composition of the outlet stream, the other operative conditions being the same: it can be observed that at high chloride concentration, when the faradic yield for the oxidation of chlorides is close to one, the concentration of chlorate is very low.

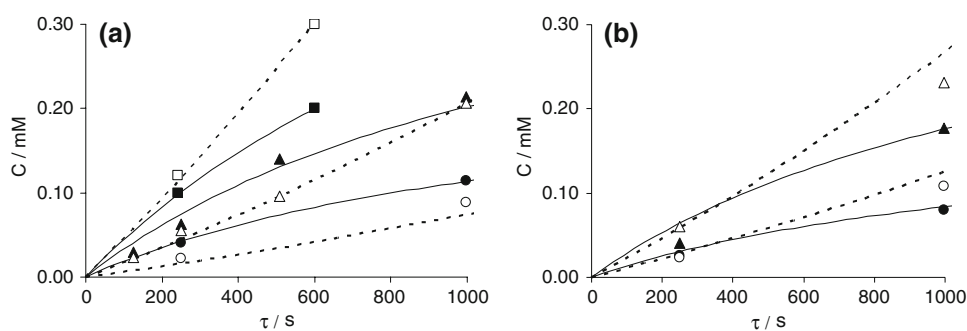


Fig. 11 Effect of the operative parameters k_m , τ and i , on the concentration of oxidants (full symbols) and chlorates (empty symbols) in the outlet stream of continuous electrolyses at BDD with

an inlet chloride concentration of 3.4 mM. $k_m = 1.2 \times 10^{-5} \text{ m s}^{-1}$ (a); $k_m = 3.0 \times 10^{-6} \text{ m s}^{-1}$ (b). $i = 2.5 \text{ mA cm}^{-2}$ (\circ ●); $i = 5 \text{ mA cm}^{-2}$ (Δ ▲); $i = 7.6 \text{ mA cm}^{-2}$ (\square ■)

Figure 9a–b shows the comparison between experimental and model predicted data at fixed residence time for diluted chlorine solutions representing a typical composition of natural waters. As can be seen the concentrations of oxidants and chlorates increase with current density and chloride concentration. It is worth to observe the effect of the mass transfer coefficient that is highlighted in the Fig. 10, in which the concentrations of hypochlorites and chlorates in the outlet stream of the reactor operating in continuous mode are showed as functions of the mass transfer coefficient values. As observed in batch experiments, also in this case the increase of the mass transfer coefficient results in a fast removal of active chlorine from the anodic zone so limiting its oxidation to chlorate by OH radicals.

Figure 11a–b summarises the combined effect of k_m , τ , i on the composition of the outlet stream, with an inlet concentration of chloride of 3.4 mM. Also in this case the proposed model well agrees with the experimental data. As can be seen an increase of the current density and residence time favours the formation of chlorates. This effect is more evident at low values of mass transfer coefficient.

4 Conclusions

Results of this work showed that at low chloride concentrations electrolysis with BDD anode produces a mixture of powerful oxidant [9, 14, 22]; although operative conditions should be carefully selected to avoid further oxidation of active chlorine to chlorate. Low current density, high values of mass transfer rate and low residence time were found as optimal conditions to maximize the concentration of oxidants and minimize the concentration of chlorates.

A mathematical model, based on a simplified reaction scheme was formulated, and the model predictions agree with the experimental data in a wide range of experimental conditions. The mathematical model may be used to predict the behaviour of electrochemical reactors for water treatment.

The proposed reaction mechanism also justifies the controversial effect of chloride ions in wastewater treatments [11, 23]: depending on the particular water, either active chlorine or OH radicals may be effective oxidants to remove the pollutant. The electrolysis with BDD in presence of high concentrated chlorides (more than 1 g/L) results in high amount of active chlorine, and low surface concentration of OH. Depending on the organic compound, and in particular on its reactivity towards active chlorine, the presence of high concentration of active chlorine may result in a positive effect, i.e. high removal rate, or in an undesired generation of chlorinated by-products.

References

- Rodrigo MA, Michaud PA, Duo I, Panizza M, Cerisola G, Cominellis C (2001) J Electrochem Soc 148:D60–D64
- Polcaro AM, Vacca A, Palmas S, Mascia M (2003) J Appl Electrochem 33(10):885–892
- Rychen P, Pupunat L, Haenni W, Santoli E (2003) New Diam Front Carbon Technol 13(2):109–117
- Polcaro AM, Vacca A, Mascia M, Palmas S, Pompei R, Laconi S (2007) Electrochim Acta 52(7):2595–2602
- Alfaro MAQ, Ferro S, Martinez-Huitle CA, Vong YM (2006) J Braz Chem Soc 17(2):227–236
- Santana MHP, De Faria LA, Boodts JFC (2005) Electrochim Acta 50(10):2017–2027
- Serrano K, Michaud PA, Cominellis C, Savall A (2002) Electrochim Acta 48(4):431–436
- Canizares P, Larrondo F, Lobato J, Rodrigo MA, Saez C (2005) J Electrochem Soc 152(11):D191–D196
- Polcaro AM, Vacca A, Mascia M, Ferrara F (2008) J Appl Electrochem 38(7):979–984
- Hastie J, Bejan D, Teutli-Leon M, Bunce NJ (2006) Ind Eng Chem Res 45(14):4898–4904
- Cabeza A, Urtiaga AM, Ortiz I (2007) Ind Eng Chem Res 46(5):1439–1446
- Greef R, Peat R, Peter L M, Pletcher D, Robinson J (1985) Instrumental methods in electrochemistry Ellis Horwood, Chichester, p 113
- Walsh F (1993) A first course in electrochemical engineering. Electrosintesis, New York

14. Sweetin DL, Sullivan E, Gordon G (1996) *Talanta* 43(1):103–108
15. Bergmann MEH, Rollin J (2007) *Catal Today* 124(3–4):198–203
16. Fierro S, Nagel T, Baltruschat H, Comninellis C (2007) *Electrochem Commun* 9:1969–1974
17. Ferro S, De Battisti A, Duo I, Ch Comninellis, Haenni W, Perret A (2000) *J Electrochem Soc* 147(7):2614–2619
18. Gandini D, Michaud PA, Duo I, Mahe E, Haenni W, Perret A, Comninellis C (1999) *New Diam Front Carbon Technol* 9(5):303–316
19. Trasatti S (1994) In: *Electrochemistry of novel materials*. VCH Publishers, New York, p 238
20. Marselli B, Garcia-Gomez J, Michaud PA, Rodrigo MA, Comninellis C (2003) *J Electrochem Soc* 150:D79–D83
21. Pourbaix M (1966) *Atlas of electrochemical equilibria in aqueous solutions*. Pergamon press, Oxford, pp 590–603
22. Bergmann H, Iourtchouk T, Schops K, Bouzek K (2002) *Chem Eng J* 85:111–117
23. Canizares P, Martinez L, Paz R, Saez C, Lobato J, Rodrigo MA (2006) *J Chem Technol Biotechnol* 81(8):352–358